

Electronic structure of Ni-based superconducting quaternary compounds: $\text{YNi}_2\text{B}_2\text{X}$ ($\text{X}=\text{B}, \text{C}, \text{N}, \text{and O}$)

J. I. Lee, T. S. Zhao,* and I. G. Kim

Department of Physics, Inha University, Incheon 402-751, Korea

B. I. Min and S. J. Youn

Department of Physics, Pohang University of Science and Technology, Pohang 790-784, Korea

(Received 19 April 1994)

In order to explore a correlation between superconductivity and the electronic structure of Ni-based superconducting quaternary compounds, a systematic investigation of the electronic structures for $\text{YNi}_2\text{B}_2\text{X}$ ($\text{X}=\text{B}, \text{C}, \text{N}, \text{and O}$) is carried out, by employing the linearized muffin-tin orbital band method. It is found that the Ni $3d$ density of states (DOS) in $\text{YNi}_2\text{B}_2\text{C}$ is broader than that in fcc Ni metal, and so $N(E_F)$ becomes small enough to make the system nonferromagnetic and then superconducting. A *rigid-band*-like shift of the Fermi level is observed as atom X varies. In the case of $\text{YNi}_2\text{B}_2\text{C}$, the Fermi level is located right at the *van Hove*-like singular DOS peak, which originates from saddle-point extremal band crossing Γ . This singular DOS peak at E_F is expected to be related to the superconductivity observed in $\text{YNi}_2\text{B}_2\text{C}$. A crude estimate within the framework of the simple rigid-ion approximation indicates that the superconductivity in $\text{YNi}_2\text{B}_2\text{C}$ can be properly described by the conventional phonon mechanism.

Following the recent report of superconductivity in Ni-based alloy systems (Y-Ni-B-C) by Nagarajan *et al.*,¹ increasing attention has been paid to synthesizing single phase samples of quaternary boro-carbides. Cava *et al.*² have synthesized $\text{LNi}_2\text{B}_2\text{C}$ ($L = \text{Y}$ and rare earths), and found that Lu and Y compounds exhibit the highest superconducting transition temperatures ($T_c = 16.6$ and 15.6 K, respectively), while compounds with magnetic rare earths exhibit lower T_c : Tm ($T_c = 11$ K), Er ($T_c = 10.5$ K), and Ho ($T_c = 8$ K). The crystal structure of $\text{LuNi}_2\text{B}_2\text{C}$ is known to be a filled variant of the body-centered-tetragonal (bct) ThCr_2Si_2 type.³ It is also found that $\text{YNi}_2\text{B}_2\text{C}$ is a type-II superconductor with the onset T_c of ~ 15 K and the Ginzburg-Landau parameter $\kappa = 10\text{--}15$.⁴⁻⁶ Hong *et al.*⁴ reported the normal state electronic specific heat coefficient $\gamma = 18.2$ mJ/mol K², the normalized specific heat discontinuity $\Delta C/\gamma T_c = 1.57$, and the low-temperature value of the Debye temperature $\Theta_D = 537$ K for $\text{YNi}_2\text{B}_2\text{C}$.

Along with the above experimental studies, Mattheiss⁷ calculated band structures of $\text{LuNi}_2\text{B}_2\text{C}$ and related intermetallic phases including LuNiBC and $\text{YNi}_2\text{B}_2\text{C}$, by using the linearized augmented plane wave (LAPW) method. His results reveal a density-of-states (DOS) peak near the top of nearly filled Ni $3d$ bands, with only modest B and C orbital mixture. Pickett and Singh⁸ also calculated the band structure, DOS, and Fermi surface of $\text{LuNi}_2\text{B}_2\text{C}$. Their calculations indicate that the material is a strongly three-dimensional (3D) metal with all atoms contributing to the metallic character, different from the case in cuprate high-temperature superconductors. They also deduced a very strong electron-phonon coupling constant, $\lambda = 2.6$, which may arise from an unusual combination of states at the Fermi level (E_F) and from vibrations of light atoms.

In this paper, we report a systematic investigation of the electronic structures for $\text{YNi}_2\text{B}_2\text{X}$ ($\text{X}=\text{B}, \text{C}, \text{N}, \text{and O}$). We have studied a change of band structures by varying the X atom in $\text{YNi}_2\text{B}_2\text{X}$. The purpose of our study is to explore a correlation between superconductivity and the underlying electronic structure which depends on the number of conduction electrons varied by X . The energy band structure and DOS are obtained self-consistently by using the linearized muffin-tin orbital (LMTO) band method and the tetrahedron method of Brillouin zone integration, respectively. The Hedin-Lundqvist form is used in the local density functional approximation for the electron-electron exchange-correlation interaction. We have used a semirelativistic band method which includes all the relativistic effects but the spin-orbit effect.

$\text{YNi}_2\text{B}_2\text{C}$ has a bct ThCr_2Si_2 -type structure with D_{4h}^{17} space group.³ ThCr_2Si_2 consists of alternating Th and Cr_2Si_2 layers, where Cr_2Si_2 layers are formed with a square-planar Cr_2 array sandwiched between the Si planes. In Cr_2Si_2 layers, a Cr atom is tetrahedrally coordinated by four Si atoms. In the case of $\text{YNi}_2\text{B}_2\text{C}$, extra C atoms are inserted in Y layers and located between B atoms connecting two Ni_2B_2 layers above and below. The crystal structure of ThCr_2Si_2 is characterized by two parameters: the free parameter z which corresponds to the location of a Si atom $(0, 0, z)$ and the c/a ratio. A typical value of z in ThCr_2Si_2 is 0.375 for the case of a regular Si_4 tetrahedron.⁹ It is found that the free parameter of the boron atom in $\text{YNi}_2\text{B}_2\text{C}$ is 0.351,⁴ which is a bit smaller than the value 0.362 in $\text{LuNi}_2\text{B}_2\text{C}$.³

We have taken the lattice parameters of $\text{YNi}_2\text{B}_2\text{C}$ to be $a = 3.5267$ Å and $c = 10.5427$ Å, as determined by Hong *et al.*⁴ For the sake of comparison, we have used the same lattice parameters for the hypothetical $\text{YNi}_2\text{B}_2\text{X}$ ($\text{X} = \text{B}, \text{N}, \text{and O}$) compounds. There is one $\text{YNi}_2\text{B}_2\text{C}$ formula

unit with six atoms in a primitive unit cell. The shortest bond length is that between B-C, which forms a linear B-C-B unit with a near-neighbor distance (d_{NN}) of 1.55 Å. Ni atoms are surrounded by four near-neighbor B atoms, with $d_{NN} = 2.07$ Å. In the square-planar Ni array, d_{NN} of Ni-Ni atoms is 2.49 Å, which is close to that of fcc Ni metal (2.50 Å). Near-neighbor distances between Ni-Y and Ni-C atoms are both 3.17 Å.

Figure 1 presents total and projected partial density of states (TDOS and PDOS) of $\text{YNi}_2\text{B}_2\text{C}$, calculated at an experimental lattice constant. The high DOS near -4 to -2 eV is due to $3d$ bands of Ni atoms, and the localized DOS around 13 eV below E_F corresponds to C $2s$ bands, in which $5p$ bands of Y and $2s$ bands of B atoms are mixed. Interestingly, in $\text{YNi}_2\text{B}_2\text{C}$, the Fermi level is located right at the DOS peak, which consists mainly of Ni $3d$ and Y $4d$ states, as seen in the projected PDOS. There is also small amount of $2p$ states of B and C atoms, which are hybridized with Ni $3d$ and Y $4d$ states (see Table I). We obtain $N(E_F) = 4.03$ states/eV, which corresponds to the specific heat coefficient, $\gamma = 9.5$ mJ/mol K². A comparison with the experimental value $\gamma = 18.2$ mJ/mol K² (Ref. 4) yields that the enhancement of electron mass λ , amounts to ~ 0.9 , which

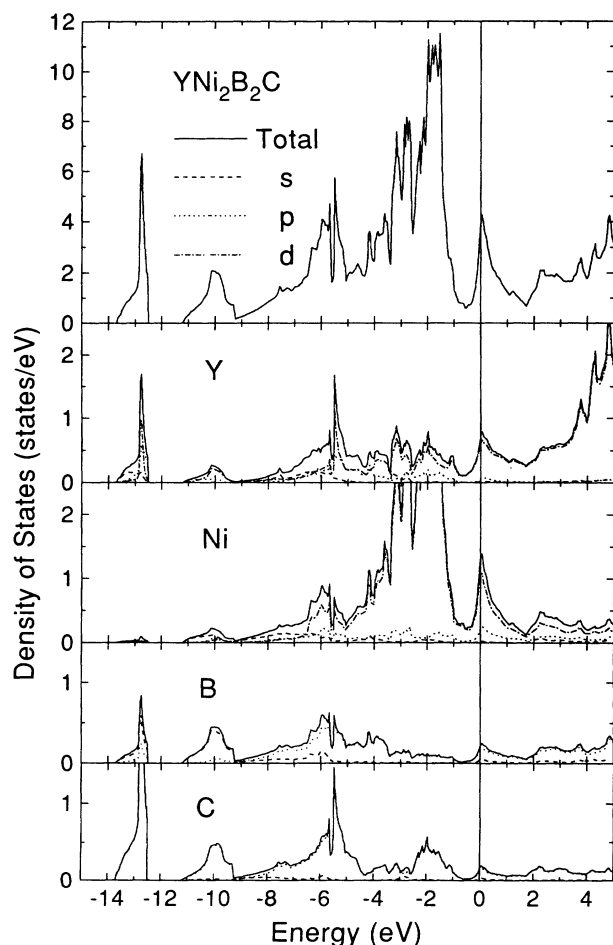


FIG. 1. Total density of states (TDOS) and angular momentum projected local density of states (PDOS) of $\text{YNi}_2\text{B}_2\text{C}$.

TABLE I. Angular momentum and site projected DOS at E_F , N_l (in states/eV), and charge occupancies Q_l of $\text{YNi}_2\text{B}_2\text{C}$. Atomic sphere radii utilized are 3.68, 2.55, 1.97, and 1.94 a.u. for Y, Ni, B, and C atoms, respectively.

	Y	Ni	B	C
N_s	0.02	0.03	0.04	0.03
N_p	0.07	0.22	0.18	0.14
N_d	0.64	1.09		
N_{tot}	0.73	1.34	0.22	0.17
Q_s	0.58	0.67	0.86	1.08
Q_p	1.18	0.87	1.58	2.48
Q_d	2.37	8.68		
Q_{tot}	4.13	10.22	2.44	3.56

is induced by the contribution from phonon or other excitations. We will discuss this point more later.

Ni $3d$ DOS in $\text{YNi}_2\text{B}_2\text{C}$ is broader than that in fcc Ni metal, due to the hybridization interaction with neighbor atoms, especially with nearest-neighbor B $2p$ states. Hybridization interactions are prominent near bonding (~ -6 eV) and antibonding (near E_F) region. Hence $N(E_F)$ becomes small enough to make the system non-ferromagnetic and then superconducting. Indeed, the Stoner parameter S , defined as $S \equiv N(E_F)I_{XC}$ with I_{XC} denoting the intra-atomic exchange-correlation integral, is less than 1 ($S = 0.44$), and so the ferromagnetic instability does not occur. Occupied charges of the Ni $3d$ band, ~ 8.7 , are close to the value in fcc Ni metal, which is contrary to Hong *et al.*'s proposal that the $3d$ band in $\text{YNi}_2\text{B}_2\text{C}$ is filled.⁴

Figure 2 shows the band structure along the symmetry lines of the bct Brillouin zone.

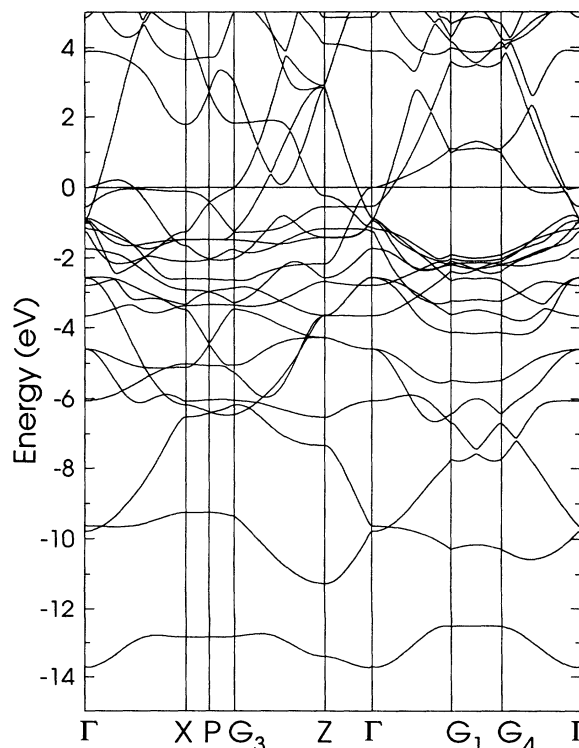


FIG. 2. Band structure of $\text{YNi}_2\text{B}_2\text{C}$ along the symmetry lines of the bct Brillouin zone.

try lines of the bct Brillouin zone. It is seen that most of bands in the z direction are flat. Dispersive bands in the z direction, e.g., the second and third bands along Γ - Z , have C $2p$ states. This fact reflects that the system would be quasi-2D-like without C atoms added, and so the carbon atoms induce $\text{YNi}_2\text{B}_2\text{C}$ to have a 3D nature. Three bands (17th, 18th, and 19th bands), which have mainly Ni $3d$ characters with small Y $4d$ states, cut the Fermi level. Hence, it is expected that electrons responsible for the conductivity are predominantly d electrons of Ni and Y atoms. A notable feature in Fig. 2 is that the 19th band at Γ crosses E_F flatly, manifesting a saddle-point extremum. This flat band produces a *Van Hove*-like DOS peak at E_F in Fig. 1, as in the case of La cuprate superconductors.¹⁰ As will be discussed below, the carbon atoms plays a role in $\text{YNi}_2\text{B}_2\text{C}$ to give rise to a saddle-point singularity at E_F . The flat band are composed of Ni $3d$ and Y $4d$ states, which reflects again the 3D nature of the system. In a sense, the nature of singular DOS peak in $\text{YNi}_2\text{B}_2\text{C}$ is not the same as in La cuprates, in which the Van Hove DOS peak originates from flat Cu-O bands in the 2D basal plane.

Figure 3 presents Fermi surfaces in the $k_z = 0$ plane of the bct Brillouin zone, which are attributed to the 17th, 18th, and 19th bands. The 17th band constitutes large hole Fermi surfaces around G_1 . There are neck Fermi surfaces along the Γ - X direction, which connect large electron Fermi surfaces centered at Γ and at X . These neck Fermi surfaces may provide open orbits in a magnetoresistance experiment. The 18th band produces a nearly spherical electron pocket centered at Γ and long *cigarlike* electron Fermi surfaces around X . An electron Fermi surface originating from the 19th band, which has a calabash shape with the axis along the z direction, is seen as a small point at Γ in the $k_z = 0$ plane. It is expected from the existence of a saddle-point singularity at E_F in $\text{YNi}_2\text{B}_2\text{C}$ that the Fermi surface topology will change very much depending on the position of the Fermi level.¹¹

DOS results for the $\text{YNi}_2\text{B}_2\text{X}$ ($X = \text{B}, \text{N}, \text{and O}$)

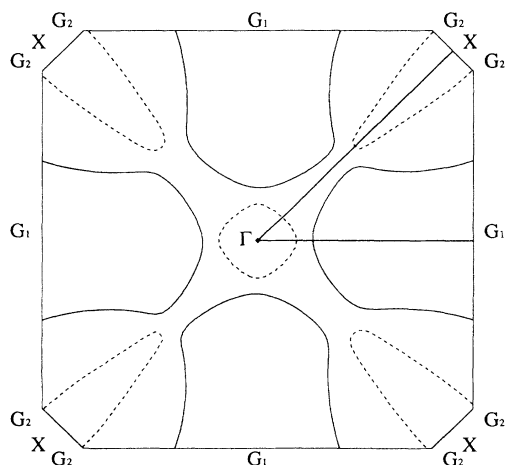


FIG. 3. Fermi surfaces of $\text{YNi}_2\text{B}_2\text{C}$ on the $k_z = 0$ plane of the bct Brillouin zone.

are given in Fig. 4. Binding energies of X $2s$ states in $\text{YNi}_2\text{B}_2\text{X}$ increase as 10, 13, 17, and 21 eV for $X = \text{B}, \text{C}, \text{N}, \text{and O}$, respectively, and even the $2s$ band of B atoms becomes split off from the main band in the case of $\text{YNi}_2\text{B}_2\text{O}$ (the O $2s$ band is not shown in Fig. 4). Prominent in Fig. 4 is the shift in the Fermi level as X varies. As compared to the DOS in $\text{YNi}_2\text{B}_2\text{C}$, E_F in $\text{YNi}_2\text{B}_2\text{B}$ is located below the singular DOS peak, while the E_F 's in $\text{YNi}_2\text{B}_2\text{N}$ and $\text{YNi}_2\text{B}_2\text{O}$ are above the peak. It is apparent that the shift of the Fermi level is *rigid-band*-like, as the number of conduction electrons increases. The value of $N(E_F)$, which is an important parameter characterizing the superconductivity, changes accordingly: 1.7, 4.0, 2.8, and 2.1 states/eV for $X = \text{B}, \text{C}, \text{N}, \text{and O}$, respectively. The comparison of DOS for $\text{YNi}_2\text{B}_2\text{X}$ thus reveals that $\text{YNi}_2\text{B}_2\text{C}$ has the highest $N(E_F)$ among $\text{YNi}_2\text{B}_2\text{X}$, and the singular DOS peak at E_F in $\text{YNi}_2\text{B}_2\text{C}$ arising from insertion of C atoms may provide a clue to the superconductivity observed in this compound.

Suppose that the whole mass enhancement $\lambda = 0.9$ comes from the phonon contribution; one obtains $T_c = 22$ K from McMillan's empirical formula¹² for T_c with the assumed Coulomb pseudopotential parameter $\mu^* = 0.13$ and the experimental Debye temperature $\Theta_D = 537$ K.⁴ This value is of the same order of magnitude as the observed $T_c \sim 15$ K.

We consider the superconducting properties of $\text{YNi}_2\text{B}_2\text{C}$, within the framework of the simple rigid-ion approximation.¹³ Calculation of $\eta_\alpha = N(E_F)\langle I_\alpha^2 \rangle$, where $\langle I_\alpha^2 \rangle$ is the average electron-ion interaction matrix element for the α atom, yields $\eta_\alpha = 0.37, 0.68, 0.37$, and

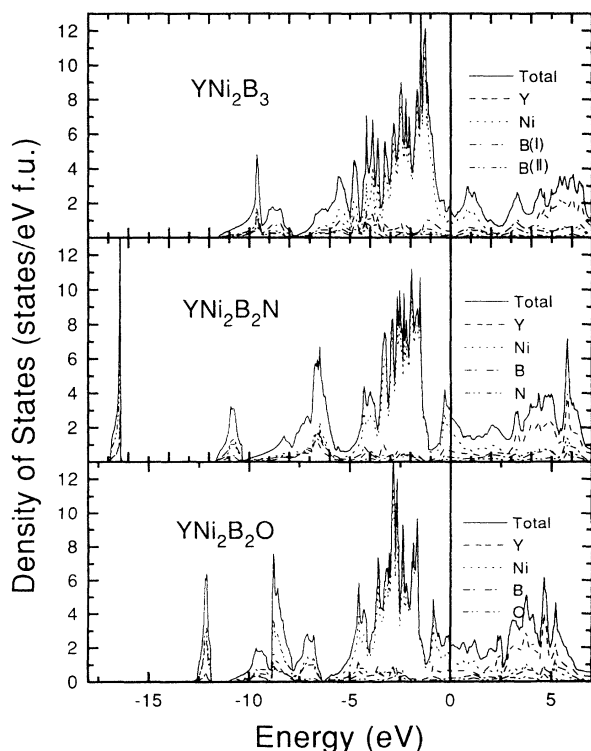


FIG. 4. Density of states of $\text{YNi}_2\text{B}_2\text{X}$, ($X = \text{B}, \text{N}, \text{and O}$). The O $2s$ band is not shown in the figure.

0.70 eV/Å² for $\alpha = \text{Y, Ni, B, and C}$ atoms, respectively. If one has information on phonon spectra, one can evaluate the electron-phonon coupling constant λ_{ph} . By using McMillan's formula $\lambda_{\text{ph}} = \sum_{\alpha} \eta_{\alpha} / M_{\alpha} \langle \omega^2 \rangle$, where M_{α} is an ionic mass and $\langle \omega^2 \rangle$ is the average phonon frequency, one obtains $\lambda_{\text{ph}} = 0.60$ for $\langle \omega^2 \rangle \simeq \Theta_D^2/2$. In fact, contributions from B and C atoms are dominating due to their light ionic masses. This feature reflects that their roles in superconductivity of YNi₂B₂C would be essential even though components of B and C bands near E_F are small. McMillan's T_c formula with $\mu^* = 0.10$ and $\Theta_D = 537$ K yields $T_c = 10.3$ K, which is again of the same order of magnitude as the observed T_c . This crude estimate indicates that the superconductivity in YNi₂B₂C could be well described by the conventional phonon mechanism. However, detailed information on phonon spectra is prerequisite for drawing a more convincing conclusion.

In summary, based on the electronic structures of YNi₂B₂X ($X = \text{B, C, N, and O}$), electronic and superconducting properties of YNi₂B₂C are investigated. We found that, in YNi₂B₂C, the Fermi level is located right at the DOS peak, which consists mainly of Ni 3d and Y 4d states hybridized with small amount of 2p states of B

and C atoms. The comparison of DOS for YNi₂B₂X reveals that YNi₂B₂C has the highest $N(E_F)$ among YNi₂B₂X. The Van Hove-like singular DOS peak at E_F , which arises from a flat band crossing Γ , is expected to provide a clue to the superconductivity observed in YNi₂B₂C. The estimate of λ_{ph} and T_c within the rigid-ion approximation indicates that the superconductivity in YNi₂B₂C can be well accounted for by the conventional phonon mechanism. Further, the roles of B and C atoms in the superconductivity of YNi₂B₂C are found to be substantial due to their light ionic masses.

This work was supported by the Korea Science Engineering Foundation through the Korean-U.S. Cooperative Science Program. J.I.L. was supported in part by the Center for Theoretical Physics of Seoul National University. B.I.M. was supported in part by POSTECH-BSRI Program of the Korean Ministry of Education. T.S.Z. acknowledges the support from the Inha University. The authors at Inha University would like to thank Dr. N. M. Hong and Professor G. Hilscher at Institut für Experimentalphysik, Technische Universität Wien for communication of their results prior to publication.

* On leave from Department of Physics, Jilin University, Changchun, China.

¹ R. Nagarajan, C. Mazumdar, Z. Hossain, S. K. Dhar, K. V. Gopalakrishnan, L. C. Gupta, C. Godart, B. D. Padalia, and R. Vijayaraghavan, *Phys. Rev. Lett.* **72**, 274 (1994).

² R. J. Cava, H. Takagi, H. W. Zandbergen, J. J. Krajewski, W. F. Pock, Jr, T. Siegrist, B. Batlogg, R. B. van Dover, R. J. Felder, K. Mizuhashi, J. O. Lee, H. Eisaki, and S. Uchida, *Nature (London)* **367**, 282 (1994).

³ T. Siegrist, H. W. Zandbergen, R. J. Cava, J. J. Krajewski, and W. F. Pock, Jr., *Nature (London)* **387**, 264 (1994).

⁴ N. M. Hong, H. Michor, M. Vybornov, T. Holubar, P. Hundegger, W. Perthold, G. Hilscher, and P. Rogl, *Physica C* (to be published).

⁵ M. Xu *et al.*, *High-T_c Update* **8** (6), 1 (1994).

⁶ B. C. Chakoumakos and M. Paranthaman, *High-T_c Update* **8** (6), 1 (1994).

⁷ L. F. Mattheiss, *High-T_c Update* **8** (4), 2 (1994).

⁸ E. Pickett and D. J. Singh, *High-T_c Update* **8** (6), 1 (1994).

⁹ A. Szytula and J. Leciejewicz, in *Handbook on the Physics and Chemistry of Rare-Earths*, edited by K. A. Gschneidner and L. Eyring (North-Holland, Amsterdam, 1989), Vol. 12, p. 133.

¹⁰ A. J. Freeman, J. Yu, and C. L. Fu, *Phys. Rev. B* **36**, 7111 (1987); J.-H. Xu, T. J. Watson-Yang, J. Yu, and A. J. Freeman, *Phys. Lett. A* **120**, 489 (1987).

¹¹ B. I. Min, S. J. Youn, J. I. Lee, T. S. Zhao, and I. G. Kim (unpublished).

¹² W. L. McMillan, *Phys. Rev.* **167**, 331 (1968).

¹³ G.D. Gaspary and B. L. Gyorfy, *Phys. Lett.* **28**, 801 (1972).